Steel and Composite Structures, *Vol. 19, No. 5 (2015) 1167-1184*
DOI: http://dx.doi.org/10.12989/scs.2015.19.5.1167

Cyclic testing of chevron braced steel frames with IPE shear panels

Seyed Mehdi Zahrai*

Center of Excellence for Engineering and Management of Civil Infrastructures, School Civil Engineering, College of Engineering, The University of Tehran, P.O. Box 11155-4563, Iran

(*Received June 26, 2014, Revised January 29, 2015, Accepted April 27, 2015*)

Abstract. Despite considerable life casualty and financial loss resulting from past earthquakes, many existing steel buildings are still seismically vulnerable as they have no lateral resistance or at least need some sort of retrofitting. Passive control methods with decreasing seismic demand and increasing ductility reduce rate of vulnerability of structures against earthquakes. One of the most effective and practical passive control methods is to use a shear panel system working as a ductile fuse in the structure. The shear Panel System, SPS, is located vertically between apex of two chevron braces and the flange of the floor beam. Seismic energy is highly dissipated through shear yielding of shear panel web while other elements of the structure remain almost elastic. In this paper, lateral behavior and related benefits of this system with narrow-flange link beams is experimentally investigated in chevron braced simple steel frames. For this purpose, five specimens with IPE (narrow-flange I section) shear panels were examined. All of the specimens showed high ductility and dissipated almost all input energy imposed to the structure. For example, maximum SPS shear distortion of 0.128-0.156 rad, overall ductility of 5.3-7.2, response modification factor of 7.1-11.2, and finally maximum equivalent viscous damping ratio of 35.5-40.2% in the last loading cycle corresponding to an average damping ratio of 26.7-30.6% were obtained. It was also shown that the beam, columns and braces remained elastic as expected. Considering this fact, by just changing the probably damaged shear panel pieces after earthquake, the structure can still be continuously used as another benefit of this proposed retrofitting system without the need to change the floor beam.

Keywords: IPE shear panel; vertical link beam; chevron braced simple frame; cyclic testing; ductility ratio; energy dissipation; response modification factor

1. Introduction

Shear panel system, SPS, or Vertical Shear Link, VSL, is a passive control method located vertically between the joint of two chevron braces and the flange of the floor beam as shown in Fig. 1. H shape or IPB sections with wide flanges are often used as a shear panel. Appearance of these pieces is like a short beam linking chevron braces to the beam. This system has stable hysteresis curves such that without causing any strength degradation or stress concentration, it can uniformly dissipate energy. SPS has high ductility in addition to having considerable stiffness. In this system,

*Corresponding author, Professor, E-mail: mzahrai@ut.ac.ir

http://www.techno-press.org/?journal=scs&subpage=8 ISSN: 1229-9367 (Print), 1598-6233 (Online)

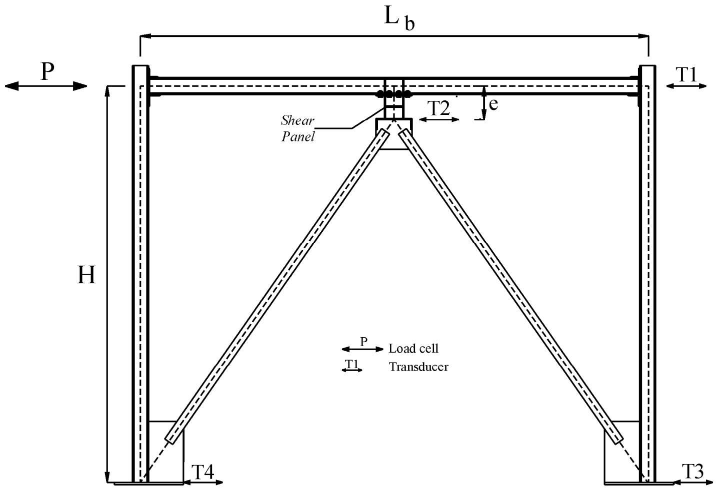

Fig. 1 Vertical shear link or shear panel system

because of suitable ductility, limited relative floor displacements and maximum displacements of buildings cannot easily cause damage in the building. Unlike Eccentrically Brace Frames, EBF, SPS as a ductile fuse is not inside of the floor slab and if connected to the main beam with bolts, it is easily exchangeable. By just changing SPS if needed, the structure can still be used after earthquake. Another main benefit of this system is its easy use in seismic retrofit of existing buildings. Overall, using SPS as an efficient method, with little expense in terms of design, construction and exchange looks promising.

If SPS is well designed, high ductility is achieved through yielding of SPS web and related seismic energy dissipation, while other elements of the structure remain elastic. Length of shear panel is one of the important parameters in designing SPS. Weaker performance of long shear panels compared with short ones has been demonstrated by several tests (Engelhardt and Popov 1992]. To have yielding in shear before bending, codes have limited the length of the shear panel to the below amount (AISC 2010, IBC 2012, CSA S16 2009).

$$e < 1.6 \frac{M_p}{V_p} \tag{1}$$

In the above formula, e is the length of SPS, M_p is capacity of plastic moment and V_p is plastic shear capacity of beam. Some researchers numerically and/or experimentally studied cyclic performance of SPS in steel frames. Fehling *et al.* (1992) numerically attempted to model shear panel for examination of stability of SPS. For this analysis, the program STABET, which offers the possibilities to investigate combined bending and torsional instability and permits introducing nonlinear behavior, has been used. Their results showed that effective stress increases due to strain hardening of up to 50% (i.e., max V = 1.5 * V_p, plastic shear-capacity). In order to achieve a certain margin of safety, calculated ductility should be larger than the required amount (defined by link shear distortion angle, γ = 0.06). According to their findings, for a 60 cm long SPS, a calculated γ value of 0.08 reflects a safety margin in ductility. To experimentally study the cyclic behavior of SPS, Bouwkamp and Vetr (1994) tested a full scale SPS frame with 3 stories and 3 spans of 5 m. Columns were arranged at minor axes to assign maximum story shear to links. Method of loading was displacement control as well as controlling the ratio of load applied to levels respectively 1/3, 2/3 and 1 at the first to third storeys. Almost all shear panel systems reached web failure synchronized at 15-20 mm. After failure of links, general and local stiffness of frame decreased seriously, but because of hardening, the strain in the links of the whole system continuously increased. Almost 90% of imposed energy was dissipated by SPS showing that all inelastic deformations occurred in the links, without other members suffering large strains such that they remained elastic. Because short shear panels permit plastic deformations and prevent buckling, moment and shear resistance can reach their maximum capacity in the link plastic zone with combination of kinematic and isotropic hardenings.

To investigate application of SPS in bridges, Zahrai and Bruneau (1999) conducted two cyclic tests on full-size girder specimens with shear panel demonstrating that these devices can possess adequate initial elastic stiffness and strength capacity to dissipate hysteresis energy. The specimens were subjected to 28 and 27 cycles of lateral loading respectively before failure occurred at 3% drift. The resulting hysteresis curves showed good dissipation while other elements remained elastic. The maximum shear distortion of both specimens was 0.12 rad, leading to link rotational ductilities of 13 and 15, respectively. The maximum curvature of both devices reached 0.25 rad/m, reflecting a curvature ductility of 8 demonstrating that the shear panels experienced significant flexural yielding in addition to their primary shear yielding.

To find out if hollow structural sections instead of wide-flange or I-shaped ones can also effectively dissipate energy as eccentrically braced frame links, Wiliams and Albermani (2003) performed a quite extensive series of tests with various thicknesses of both single and double diaphragm plates on square hollow section (SHS) with dimensions of 100 mm. No buckling or failure occurred at cap beam displacement of up to 30 mm and all specimens had open stable hysteresis loops until 40 mm. Thinner diaphragms obtained a ductility of 20, while the ductility of thicker ones was between 10 and 15. In all cases, the ductility of frames was around 8. Diaphragms withstood maximum shear strain around 11.8 to 24.2% without failure. Berman and Bruneau (2007) also conducted an experimental and analytical investigation to use hollow rectangular cross-sections instead of wide-flange or I-shaped ones as SPS in eccentrically braced frames. These specimens in contrast to I-shaped cross-sections do not essentially require lateral bracing. Very short links have large stiffness and thus large base shear forces should be provided. So longer links, still maintaining shear behavior were used. Link was designed in a way that flange or web buckling would not occur. Compactness of flange and web in addition to stiffener spacing was checked according to the AISC Specification and the tests proved that these specification are efficient. The yield drift and the corresponding base shear were identified as 0.37% and 668 kN while maximum drift and base shear were 2.3% and 1009 kN respectively. The yield rotation and link shear at yield were 0.014 rad and 490 kN while the maximum rotation and link shear were 0.151 rad and 740 kN respectively. Fracture initiated in the heat-affected-zone adjacent to the fillet weld used to connect the stiffener to the flange.

In order to have a smaller yield deformation to achieve higher ductility and more shear stiffness, Saedi Daryan *et al*. (2008) used a finite element method for braced frames with shear panels made of Easy-Going Steel, EGS, instead of constructional steel, CS. Since yield stress is lower in EGS, more brace section area is required hence the potential of flange and web buckling is decreased. They conducted a pushover analysis on selected 4, 8 and 12-story frames with EGS shear panels under earthquake loads. Every frame was loaded until 3% drift. Shear panels dissipated over 95% of the total energy although EGS did not have much influence on reducing displacement in 8 and

12-story frames because EGS only affects shear displacements while in tall structures, bending displacements have a considerable role.

De Matteis *et al*. 2008 conducted an extensive series of experimental and numerical studies testing the behavior of aluminum alloy stiffened shear panels as a passive seismic device being able to dissipate a large amount of energy. A good agreement was observed between experimental and numerical results to model the behavior of device. Özhendekci and Özhendekci (2008) designed 420 EBFs with shear links, 105 EBFs with intermediate links, and 105 EBFs with moment links and performed inelastic dynamic analyses using DRAIN-2DX to investigate the effects of the geometry selection on the frames' seismic behaviors and weights.

Hossain *et al*. (2009) used a decomposed kinematic hardening rule to simulate nonlinear material behavior in modeling Yield Shear Panel Device, YSPD as a small, inexpensive and easy to install device. The basic point was to concentrate the inevitable structural damages to YSPDs and hence keeping the main structural components intact. Based on their findings, the simplicity of YSPD allows the damaged devices to be replaced by the new ones without any major structural reconstruction. Hossain *et al*. (2011) used a theoretical approach to predict the initial stiffness of (YSPD) compared with both experiments and developed FE models analyzed by ANSYS. YSPD relies on the in-plane shear deformation of a thin diaphragm steel plate welded inside a square hollow section (SHS). SHS as a boundary element causes tensile strips to be formed and the tension field to be developed following the post-buckling of the thin diaphragm plate. Because of large displacement in the diaphragm plate, most earthquake energy would be dissipated by plastic deformation.

In order to carefully understand the link behavior at different levels of nonlinear deformations, Zahrai and Moslehi Tabar (2013) developed an extended mathematical model for evaluation of lateral stiffness of braced frames having SPS. They proposed a mathematical expression to select the geometric properties of the SPS regarding the desired ductility and found that, the ultimate plastic lateral deformation is directly proportional to the link length, and a deteriorating coefficient accounts for the stress triaxiality effect. According to their proposed relation, the SPS geometric properties may be pre-selected regarding the desired plastic deformation.

In another research using aluminum SPS, Rai *et al*. (2013) conducted a shake table study of a single-bay two-story 1:12 reduced scale model of an aluminum shear-link enabled braced frame to evaluate the performance of shear-links as energy dissipation devices. The test indicated that the frame attracted about 41-64% less base shear compared to ordinary CBF for varying PGA levels of the ground motions. Significant amount of energy was absorbed by aluminum shear-links leading to satisfactory response up to the scaled PGA of 1.7 g, while the CBF frame could not survive the scaled PGA of 0.8 g.

While in most previous research projects, box sections or wide flange H-shaped with ductile steel sections as the link beams or ADAS and TADAS plates were tested in braced moment resisting frames, in this research IPE steel sections constructed with typical existing steel with higher yield stress than those usually proposed, implemented in chevron braced simple steel frames having angle beam-column connections are tested. The wide flange sections are more expensive and less available than IPE sections in some countries like Iran where the positive results of this research can increase the usage of such ductile systems with lower cost and more ordinary facilities. It is shown that even typical IPE section link beams can improve behavior of steel structures without the need for lateral support. Finally, a castellated beam as floor beam of the SPS chevron braced is used to investigate the efficiency of the shear panel system connected to castellated beams.

The experimental program in this research aims to show that typical narrow-flange IPE sections can be used for designing new steel buildings and retrofitting of existing buildings with simple frames. For this purpose, five specimens are tested to show the ability of dissipating earthquake energy and to display their high ductility.

2. Experimental program

2.1 Test set up

To investigate the cyclic performance of the chevron braced steel frames with IPE link beams, five specimens of shear panels were examined. Tests were conducted in structural laboratory of the Building and Housing Research Center in Tehran/ Iran. Hydraulic actuators were mounted on top of the frames and along the centerline of the beams to apply cyclic loading. Fig. 2 shows the test set up, specimen details and SPS cross sections. From one side, two hydraulic jacks were linked to electro pumps by related pipes and from the other side the system was linked to data logger machine. Using this system, the input forces and induced displacements, could be exactly recorded. Strain gauges were installed on both chevron braces, the web of the shear panel and also the panel zone located on horizontal beam to enable axial and shear forces and also shear distortion and device rotation to be determined (Fig. 2(a)). The specimens were also whitewashed as shown in Fig. 2(c) to help recognize yielding in shear panels, panel zones, braces and columns. It would be noticeable that as columns and braces were designed to remain elastic, no yielding in those elements was observed.

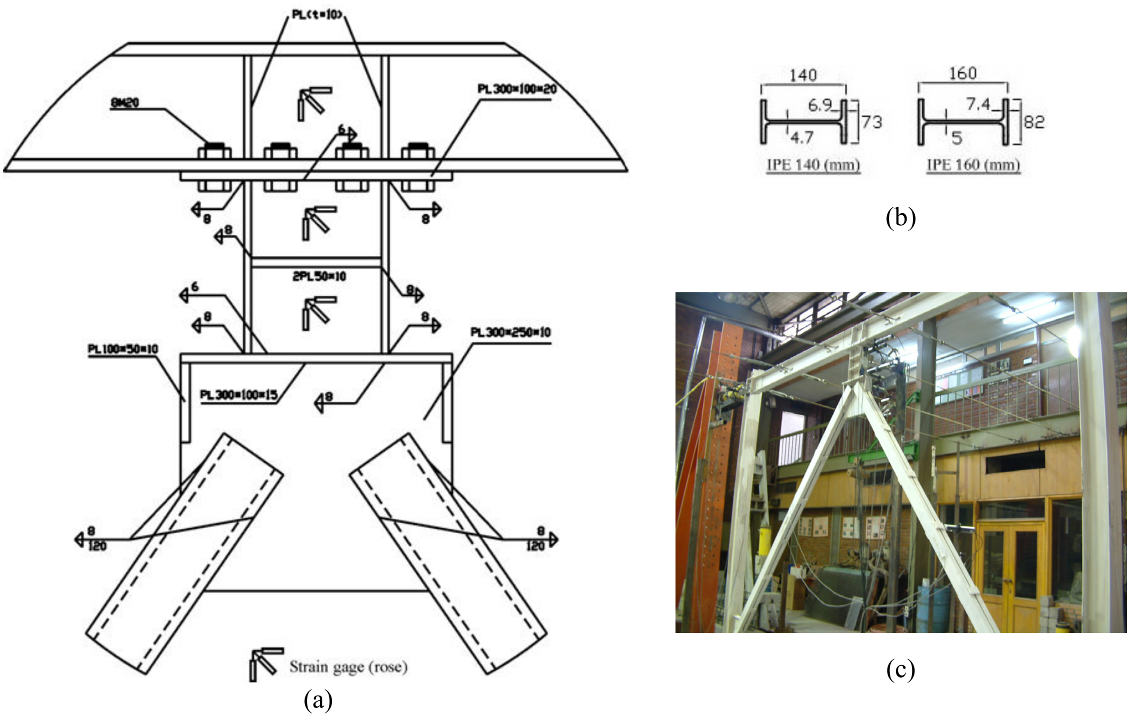

Fig. 2 (a) Location of instrumentation; (b) SPS IPE cross sections; (c) Test set up and specimen

Table 1 Properties of test steel frames having shear panels

Specimen	Frame properties						Shear panel properties			
	Column section	Column height (cm)	Beam section	Beam length (cm)	Brace section	Brace length (cm)	Shear panel section	Link length (cm)	Stiffener thickness (mm)	Stiffener distance (cm)
SPS1	IPB120	300	IPE140	420	2UNP80	345	IPE160	20	10	10
SPS2	IPB120	300	IPE140	420	2UNP80	345	IPE140	20	10	10
SPS3	IPB120	300	IPE140	420	2UNP100	345	IPE140	20	-	-
SPS4	2IPE140	300	IPE180	420	2UNP80	337	IPE140	30	10	10
SPS5	2IPE140	300	CPE180	420	2UNP100	337	IPE160	30	10	10

Table 2 Characteristics of steel materials in shear device of tested specimens

Name of specimens	F_y (MPa)	F_u (MPa)
SPS 1	280	420
SPS 2	337	482
SPS 3	361	5080
SPS 4	364	517
SPS 5	358	5130

2.2 Test specimens

Five specimens were prepared on frames with shear panels according to the AISC-LRFD 2010 code and related seismic provisions. Since designing a single floor and single-bay frame under real loads usually results in little sections for structure elements, it was decided that by presuming details of shear panel, other elements would be designed proportional to the shear capacity of the shear panels. In Table 1, details of the frames and shear panels of five specimens are given.

Angles were used at the beam-column connections to have simple frames. Connection of the beam to the shear panel was kind of friction bolted connection and for this purpose, 8 high-strength bolts of A325-M20 were used. To further simplify replacement of SPS, bolts can be used for connecting the braces to the gusset plate. For comparing different curves, yield stress was needed. Hence, steel coupons were tested to obtain details of steel materials for experimental specimens as presented in Table 2.

2.3 Instrumentation

The frame subassemblies were extensively instrumented. Instrumentation included load cells for imposed lateral forces, displacement transducers for global frames and SPS in-plane and out-of-plane displacements as shown in Fig. 1 and Fig. 2(c), and strain gauges (KFG1011) to allow subsequent determination of frame stresses and forces. Strain gauges (YEFLA5, 2) were also included in the SPS to show its inelastic behavior. To measure rate of strain in different parts of the specimens, 27 elastic and plastic strain gages were used. From these strain gages, 6 were elastic and others were plastic. To control the strains and axial forces in columns, 6 elastic strain gages were fixed on the flanges and web of the columns. Also to record rate of axial force on the braces and control the situation of local yielding and ultimately obtain the shear force in shear panel, 4 strain gages were used in the sides of the braces. Moreover, some strain gages were used in the most critical part of the specimen that is the shear panel. In each panel zone, rosettes (3 strain gages with angles 0, 45 and 90 degrees) were placed. Also on the flanges of each shear panel, 4 strain gages were fixed. To control the situation of yielding in the beam at the connection to the shear panel, 7 plastic strain gages in total were installed including one rosette (3 on the panel zone with angles 0, 45 and 90 degrees) and 4 on the stiffeners, further details of the strain gages are shown in Fig. 2(a).

2.4 Test frame lateral support

To prevent out-of-plane movement of the frame, some number 10 bars were used to horizontally anchor beam upper flange to a fixed support. According to Fig. 3, these anchor bars were installed on both sides of the frame and at specified distances, (according to the rate of force). All specimens were instrumented for displacement and strain measurements at critical points. They were also whitewashed to display yielding and their failure progress. Two reaction frames were used to support the end of horizontal actuators used to apply lateral loads to the specimens.

Fig. 3 Preventing out-of-plane movement of frames

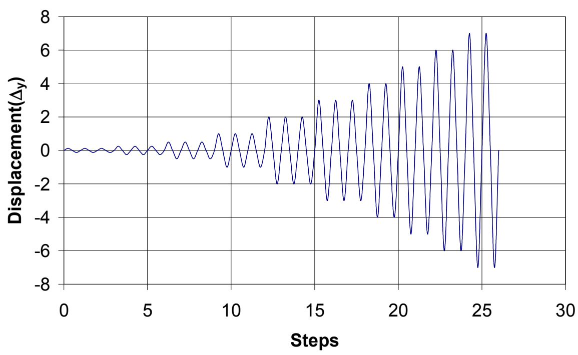

Fig. 4 Applied lateral displacement to frames

2.5 Lateral loading

The quasi-static loading protocol used here was developed based on the guidelines presented in AISC (2010) Seismic provisions. The story drift sequence was applied by two single-action 1000 kN actuators running in alternation. In order to assess a reasonable value of yielding displacement, force-control load history was applied to the test frame before appearance of yielding on the SPS member. According to AISC 2010 (seismic provision), loading cycles were determined orderly 0.125, 0.25, 0.5, 1, 2, and $3\Delta_y$, each of them 3 cycles, and from $4\Delta_y$ to specimen rupture, 2 cycles were applied by displacement control as shown in Fig. 4.

But in the laboratory situation because of having slip in the hinged support, it was difficult to reach the desired displacement in little deflections. So before the stage of specimen yielding, the test was conducted by force control according to related displacements applied in 3 cycles. After specimen yielding, displacement control was adopted for lateral loading and test was continued accordingly.

3. Test results & observations

Observations in different tests were similar to a great extent. First, specimens were covered with a layer of whitewash. When the test frame was subjected to cyclic loads, by increasing the lateral loads up to yielding limit, the whitewash cover started to crack. Of course this was only a signal and for measurement assurance, the strain gage data were used. By observing the signs of yielding in the shear panel web, yield force and yield displacement were estimated and the test was subsequently continued in displacement control.

After yielding of the shear panel web, frame lateral stiffness decreased. With increasing the applied displacement to the test frame, the web of the shear panel gradually entered the plastic phase and became a parallelogram as shown in Fig. 5. Other elements remained perfectly elastic, such that the frame was simply used for the next tests, although in the first test at some spots of the braces, minor cracks were observed as shown in Fig. 6. These cracks probably appeared because connections of the braces were not perfectly hinge or because of induced large lateral deformations, at which small bending moments were established in the brace connections.

Fig. 5 Removal of all whitewash cover in panel zones of shear panel (as the only lateral load resisting system) and deformation of shear panel into a parallelogram shape due to inelastic shear distortion

Fig. 6 Local yielding of braces because of bending moment formation in one end at the 26th cycle corresponding to 24 mm lateral displacement or $4\Delta_y$ for SPS1

Fig. 7 shows that in the past cycles, the flange of the shear panel to some degree encountered local buckling and yielding as well and its web faced large inelastic deformations until the test was stopped at last at web shear rupture. In third specimen having no stiffener, under applied inelastic large deformations, the web of the shear panel buckled as shown in Fig. 8. Fig. 9 shows that at the end of this test, the web of SPS ruptured diagonally. Also in the 4th test at large deformations, the flange of the shear panel yielded and buckled as shown in Fig. 10. Flange yielding is observed in Fig. 11 at the 13th cycle corresponding to $3\Delta_y$ for SPS5 connected to a castellated beam.

Fig. 7 Complete rupture of shear panel section in specimen 2 at the 26th cycle corresponding to 38.5 mm or $7\Delta_y$

Fig. 8 Buckling of the un-stiffened shear panel web (SPS3) under large deformations

Fig. 9 Diagonal tearing of the shear panel web at the end of third test with no stiffener

Fig. 10 Yielding and buckling of shear panel flange of SPS4 at 18th cycle corresponding to 21 mm lateral displacement or $3\Delta_y$

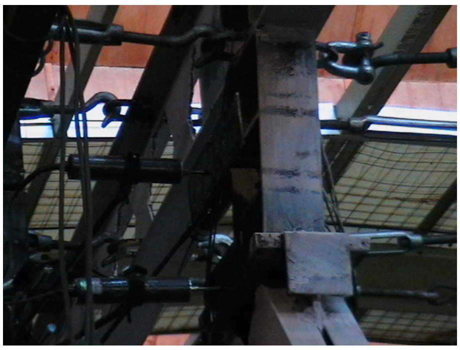

Fig. 11 Flange yielding of SPS5 connecting to castellated beam at the 13th cycle corresponding to $3\Delta_y$

Force-displacement hysteretic curves of the 1st to 5th frame specimens are shown in Fig. 12. The frame subassembly overall demonstrated very good behavior through the entire sequence of cycles and before failure of the test frame. The frame peak forces are extremely consistent in opposing directions as well as from cycle to cycle, implying similarly consistent behavior for reversed loading. The frames of the first 3 specimens were similar to each other while the other 2 specimens were identical in terms of their frame members. Meanwhile, lengths of the shear panel in the first to third specimens were 20 centimeters but in the 4th and 5th specimens were 30 centimeters. So curves of similar frames were plotted in one figure to have a better comparison. According to these figures, all specimens have large and stable hysteretic curves with high energy dissipation capacity. Because of combination of kinematic and isotropic hardenings, ultimate strength to yielding strength in these tests reached to values near 2.

As shown in Fig. 12(a) for the 1st SPS, evidence of yielding became apparent on the shear panel at about 100 kN lateral force corresponding to 6.3 mm top lateral displacement (4.5 mm net displacement after deducting slip at the bearings). Yield force was calculated as 120 to 140 kN for the 1st to 3rd SPS following the interception of the load-displacement curve and a line parallel to the initial stiffness drawn at 0.2% strain. In the 23rd cycle at 18mm lateral displacement or $3\Delta_y$, the shear panel turned into a parallelogram shape due to inelastic shear distortion as shown in Fig. 5. During the 26th cycle corresponding to 24 mm lateral displacement or $4\Delta_y$ for SPS1, as shown in Fig. 6, local yielding of braces was observed because of bending moment formation in one end of the braces. Finally, in the 29th cycle at the top lateral displacement of 36 mm or $6\Delta_y$, the SPS1 test was terminated due to tearing on the web of shear panel close to its bottom connection.

The maximum link shear force and shear distortion were 210-220 kN and 0.129-0.146 rad, respectively as shown in Fig. 12(b) for the 4th and 5th SPS specimens. Note that the current shear distortion limit for shear links in EBFs is 0.08 rad based on AISC2010. There was no evidence of crack initiation in welds or any sign of failure in other members. Taking projections of the elastic

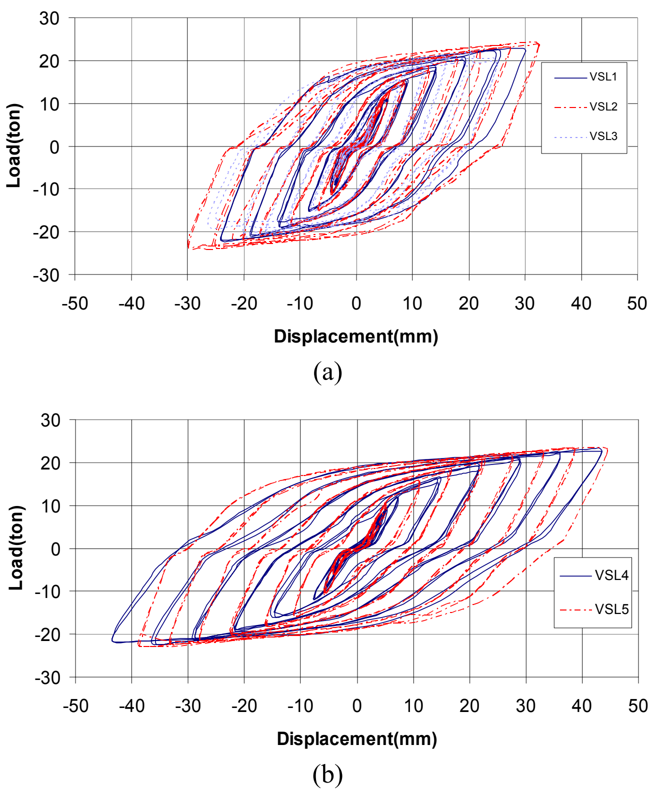

Fig. 12 Force-displacement hysteretic curves for: (a) the 1st to 3rd specimens; (b) the 4th and 5th specimens (1 ton = 1000 kg)

and inelastic slopes of Fig. 12(b) into consideration, the modified yield lateral force was approximately 120-140 kN corresponding to lateral displacement of 6-6.2 mm. The maximum base shear and displacement were 220 kN and 44 mm, respectively. Due to 3 m height of the frame, this maximum displacement was corresponding to near 1.5% drift. Therefore, the ductility ratio of SPS4 and SPS5 was obtained about 7.

Using these curves, ductility factors of the frames with shear panels were obtained between 5.2 and 7.5. Of course 5.2 is related to the specimen with no stiffener, and 6 is related to the specimen in which weld of shear panel to the upper beam was ruptured. Apart from these two specimens, ductility factor of frames was obtained between 6.9 and 7.5 showing less discrepancy and more compatibility.

4. Determination of reduction factor

To determine the reduction factor or response modification factor, the formula below was used

$$R = R_{\mu} \,.\, \Omega \,.\, Y \tag{2}$$

In which, R is the reduction factor of structure, R_{μ} is the real reduction factor due to ductility, Ω is the over strength coefficient and Y is the allowable stress factor. R_{μ} is a function of structure lateral period, T, total ductility factor of structure, μ and kind of the soil. Ω, over strength coefficient, as a result of redistribution of internal forces, strain hardening, influence of strain rate is related to the factors such as kind of structural system, shape of the structure, number of stories, etc. Y, allowable stress factor is used for considering differences in the pattern of codes in designing with the limit state method or the permissible-stress method (Miranda 1993). The total ductility factor of structure, μ is equal with the ratio of maximum displacement, Δ_{max} to equivalent yield displacement, Δ_y.

$$\mu = \frac{\Delta_{max}}{\Delta_y} \tag{3}$$

Ω is the storage resistance between the first real level of yielding, C_y and the first level of considerable yielding, C_s, that their quantities are obtained from force-displacement curves of the frames as typically shown in Fig. 13.

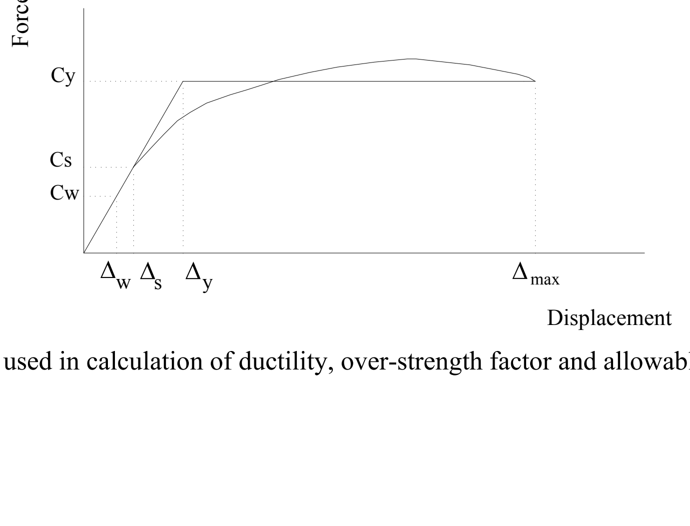

Fig. 13 Parameters used in calculation of ductility, over-strength factor and allowable reduction factor

Table 3 Computed reduction factor for each test specimen

Specimen name	Δ_{max} (mm)	Δ_y (mm)	μ	R_μ	C_y (ton)	C_s (ton)	Ω	Z (cm^3)	S (cm^3)	Y	R
SPS1	26.9	4.5	6.0	3.27	22.64	9.48	2.39	123	109	1.41	11.0
SPS2	29.5	4.3	6.9	3.54	23.72	7.76	3.06	88	77.3	1.42	15.4
SPS3	21.9	4.2	5.2	2.64	19.82	7.52	2.64	88	77.3	1.42	9.9
SPS4	39.6	5.3	7.5	3.62	22.94	9.09	2.52	88	77.3	1.423	13.0
SPS5	41.5	5.6	7.4	3.57	23.15	7.33	3.16	123	109	1.41	15.9

$$\Omega = \frac{C_y}{C_s} \tag{4}$$

Y is equal to the proportion of the first level of considerable yielding, C_s, and the related level of the design force, C_w.

$$Y = \frac{C_s}{C_w} \tag{5}$$

According to the AISC code, this factor is equal with

$$Y = \frac{ZF_y}{S(0.6F_y(\frac{4}{3}))} = \frac{1.25Z}{S} \tag{6}$$

Where Z and S are plastic and elastic section modulus respectively. Using the above method, reduction factor of each specimen is computed and shown in Table 3. It is necessary to note that obtained amounts are computed after elimination of the slip in force-displacement curves. As it is shown, the reduction factor of the specimens varies between 7.1 and 11.2.

As mentioned before, in the first specimen because of weld rupture between the shear panel and the upper beam, the full capacity was not achieved. The 3rd specimen had no web stiffener and thus sustained less ductility. Except these two specimens, the reduction factor of the other specimens was computed between 13.0 and 15.9, having more compatibility. Although the seismic provision of AISC 2010, for frames without moment connections at columns away from link, presents the reduction factor equal to 7, it seems that for these structures, larger reduction factors of around 9 to 10 are conservatively more logical.

While the reduction factor of 13.0 is related to IPE140 with a length of 30 centimeters and considering that for shear behavior dominance, the maximum allowable length for IPE140 is 39 cm, its shear yielding dominance was decreased a little. But for a length of 20 cm, where the reduction factor for the specimen without a stiffener is 9.6 and for a specimen with a stiffener is 10.1, it is shown that the reduction factor of the shear panel with a length of 20 cm without stiffener is more than the reduction factor of the shear panel with a length of 30 cm and with a stiffener. Also frame reduction factor with shear panel of IPE160 section and length of 30 cm is 11.2 (Maximum allowable length for IPE160 section is 45 cm). So it is shown that the behavior of shorter shear panels (that work in shear inelastic mode) compared with long link beams is more satisfactory. For using the maximum capacity of shear panels, it is recommended to prevent the length of these pieces from becoming close to the maximum allowable limits in design codes mentioned in part 2.

In the test of the fifth specimen, it was decided to use a castellated beam as the floor beam for checking the efficiency of the shear panel system when connected to castellated beams. For this purpose, the castellated beam was used having 2 stiffeners in the panel zone with a thickness of 6 mm. As shown in Fig. 12 and also Table 3, if the web of a castellated beam is stiffened, its use has no negative effect on the hysteretic behavior of specimen.

5. Energy dissipation & equivalent damping coefficient

Hysteretic damping or the dissipated energy in each cycle is shown by area A_h in Fig. 14. Equivalent viscous damping ratio with this area is (Priestly *et al.* 1996)

$$\xi_{eq}=\frac{A_h}{2\pi V_m \Delta_m}=\frac{A_h}{4\pi A_e} \tag{7}$$

In the above formula, V_m is the average of maximum forces (push-pull), Δ_m is the average of the maximum displacements (push-pull) in the force-displacement curve. A_e is the area of potential energy in a linear elastic system under elastic situation and with effective stiffness K_{eff}.

$$K_{eff}=\frac{V_m}{\Delta_m} \tag{8}$$

It is obvious that the maximum damping ratio is obtained from Eq. (7) for an elastic-perfectly plastic system. In such a system like pure coulomb friction behavior, area of dissipated energy in each cycle, A_h, is the area of a rectangle whose one side is equal to total force of pull-push in the structure, $2V_m$, and the other side is total maximum displacement of the structure, $2\Delta_m$. So $A_h = 4V_m*\Delta_m$ and according to the above formula, maximum damping ratio for such a system is

$$\xi_{eq}=\frac{2}{\pi}=0.64 \tag{9}$$

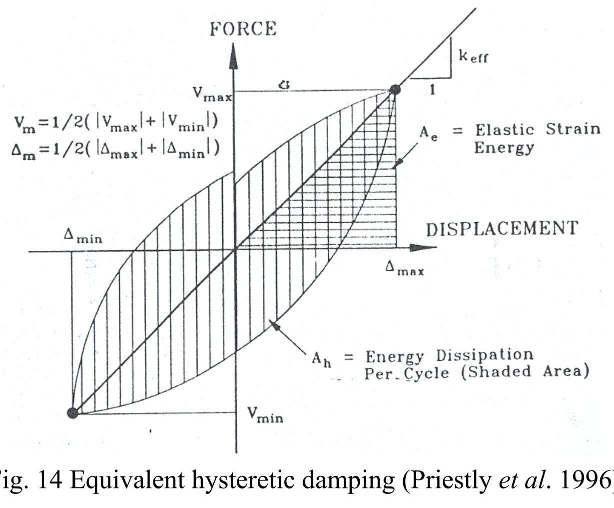

Fig. 14 Equivalent hysteretic damping (Priestly *et al.* 1996)

Table 4 Equivalent viscous damping coefficient in last cycle of specimensd

Specimen name	A_h (kg.m)	$V_{\max}$ (kg)	$V_{\min}$ (kg)	V_m (kg)	$\Delta_{\max}$ (mm)	$\Delta_{\min}$ (mm)	Δ_m (mm)	ξ_{eq} (%)
SPS1	1248	22494	22093	22293	25.58	24.08	24.83	35.9
SPS2	1743	24342	23280	23811	32.40	29.86	31.13	37.4
SPS3	1222	20366	18632	19499	25.04	26.24	25.64	38.9
SPS4	2175	23291	21910	22000	43.13	43.17	43.15	35.5
SPS5	2210	23113	22645	22879	38.30	38.60	38.45	40.2

Table 5 Equivalent damping coefficient in shear panel specimens in other inelastic cycles (%)

Specimen name	$2\Delta_y$	$3\Delta_y$	$4\Delta_y$	$5\Delta_y$	$6\Delta_y$	$7\Delta_y$	Average
SPS1	16.6	25.0	31.0	34.2	-	-	26.7
SPS2	12.9	21.6	27.3	31.4	33.3	36.3	27.1
SPS3	14.9	24.1	29.0	34.5	40.2	-	28.5
SPS4	20.1	24.3	28.7	31.8	34.8	-	27.9
SPS5	18.7	26.0	30.4	33.7	36.2	38.8	30.6

Practically obtaining this amount of equivalent damping is almost impossible. For steel structures, the rate of damping is estimated from 2 to 5% of the critical damping. But for concrete structures this rate is between 2 and 7%. In Table 4, amounts of equivalent viscous damping ratio for the experimental specimens in the last loading cycle are shown. For other loading cycles, average of damping ratio for 5 above specimens were computed, similar to the above method, and are available in Table 5.

As presented in Tables 4 and 5, the maximum equivalent viscous damping ratio of this system reached values from 35.5 to 40.2% and average of this ratio reached 26.7-30.6%. While damping of concrete and steel structures is usually less than 5%, reaching this amount of damping shows that the designed damping system is very efficient and has a high capacity to absorb and dissipate seismic energy.

In Fig. 15, hysteretic behavior of shear panels of the first to fifth specimens is shown, all of which demonstrate more than 95% contribution of SPS in resisting lateral loads. The maximum shear force reached 210 to 230 kN for the 1st to 3rd specimens as shown in Fig. 15(a) corresponding to local ductility values of 21 to 32 and shear distortion angles of 0.128 to 0.133 while codes limit this angle to 0.06 to 0.09 rad for shear links. The lowest degree of ductility was observed for the 3rd specimen where intentionally no web stiffeners were used for the SPS. The maximum shear force reached about 215 kN for the 4th to 5th specimens as shown in Fig. 15(b) corresponding to local ductility values of up to 18 and shear distortion angles of 0.129 and 0.146. It is obvious that local ductility reduced with increasing the link length.

Note that in Fig. 15, the lateral force of the SPS was measured using the total horizontal components of axial forces in the chevron braces. Axial forces of the braces were in turn obtained using their strain data as indicated in Sec. 2.3. The shear distortion angle was also obtained by dividing the lateral deformation in the SPS by its length.

Bolted supports, connecting both columns to the strong floor of the structural laboratory caused a little slip at column supports throughout the tests. This slip led to a slight pinching in the overall hysteretic behavior of specimens, as observed in Fig. 12. However, this pinching is not observed in the hysteretic behavior of shear panels in Fig. 15, as it was obtained using shear load versus shear distortion (both for just the shear panel), which is not affected by little slip of the frame at its base.

6. Technical interpretation of other results

As shown in Fig. 15, all the specimens have large and stable hysteresis curves in a ductile manner without any sign of pinching and/or degradation. Comparing the force-displacement curve with the hysteretic curve of the shear panel, it becomes clear that almost all of the lateral force imposed to the frame is tolerated by the shear panel. With this system, frames do not necessarily require rigid connection between beams and columns. Columns axial forces did not exceed more than 16 kN that was much less than the required magnitude for yielding the sections. Also axial force in braces remained less than half of the similar axial force of their yielding. So tests have shown that the experimental specimens are so efficient for dissipation and absorbing seismic energy and the expectation that other parts remain elastic is practically met.

Also the maximum shear distortion of SPS reached large amounts as these pieces work in shear mode they can show high ductility capacity. Local ductility of shear panel pieces could reach up to 30 for short SPSs. As shown in this paper, with increasing the length of the shear panel segment, the ductility of these pieces decreased. SPS4 specimen is made of IPE140, and SPS5 specimen is of IPE160 while they both are 30 cm in length. But the length of the 5th specimen has a higher distance from its allowable rate causing its ductility to be larger than that of the 4th specimen.

7. Conclusions

To investigate the effect of using shear panels in dissipating imposed cyclic energy to the structure, 5 specimens of single-story single-bay frames were designed and tested in this research. Chevron braced simple steel frames with shear panels of IPE steel section constructed with typical existing steel with higher yield stress than those usually proposed, were considered. It was shown that even typical IPE section link beams could improve the behavior of steel structures having simple beam-column connections without the need for lateral support. Finally, a castellated beam as the floor beam of the SPS chevron braced was used to investigate the efficiency of shear panel system connected to castellated beams.

In all specimens shear distortion of SPS before rupture reached 0.128-0.156 rad. All specimens sustained large and stable hysteresis curves with no pinching. Using web stiffeners, by preventing web buckling, led to larger ductility and better behavior of specimens.

Because of combination of kinematic and isotropic Hardening, the ratio of ultimate strength to yield strength in these tests reached about 2. Frame ductility of the specimens was obtained in the range of 5.2 to 7.5 that show high ductility of these pieces. Also the reduction factor of the specimens was computed between 10 and 16. It seems that for SPS, using the reduction factor between 9 and 10 is conservatively more logical. In all of the specimens, almost all of the input energy applied to the structure was dissipated by the shear panel as the passive control. Average equivalent viscous damping ratio in the inelastic cycles reached 26.7-30.6% showing a high dissipation of the cyclic energy by these pieces. Short shear panels having shear behavior showed better performances than long shear panels with flexural behavior.

Ductility of the structure increased using SPS that dissipated the imposed energy as a ductile fuse in the structure and prevented yielding of other elements of the frame like the beam, column and brace. Based on test results, the rigid connections between beams and columns are not necessary when using this system. Using bolts for connecting the shear panel to main beam and braces, SPS can be easily exchanged after earthquake and are considered as a disposable system. Since ductile behavior is expected from the shear panel, these pieces must be made of mild or low yield steel.

Shear panel system is one of the most effective and useful systems of hysteretic or metallic dampers which are easily applicable. Considering that shear panel is outside of the main frame, one of its important benefits is its usage in seismic retrofit of the existing buildings having simple beam-column connections. However, to enable the use of such IPE sections in practice, further numerical/experimental work is recommended on a wider range of specimen sizes.

Acknowledgments

This research forms parts of projects sponsored by the college of Engineering at the Univ. of Tehran (project 8108020/1/06) and the Building and Housing Research Centre (BHRC) through Grant 1-4560. Their supports are gratefully acknowledged by the author. Any opinions presented in this paper, however, are the author's alone, and not necessarily the sponsors'.

References

American Institute of Steel Construction (2010), Seismic provisions for structural steel buildings; AISC Chicago, IL, USA.

Berman, J.W. and Bruneau, M. (2007), "Experimental and analytical investigation of tubular links for eccentrically braced frames", *Eng. Struct.*, **29**(8), 1929-1938.

Boukamp, J.G. and Vetr, M.G. (1994), "Design of eccentrically braced test frame with vertical shear link" *Proceeding of the 2nd International Conference on Earthquake Resistant Construction and Design*, Berlin, Germany, June.

CSA S16 (2009), Design of steel structures, (Including Update No. 1 (2010), Update No. 2 (2010), Update No. 3 (2013)), Standard published by CSA group; Willowdale, ON, Canada.

De Matteis, G., Formisano, A., Panico, S. and Mazzolani, F.M. (2008), "Numerical and experimental analysis of pure aluminum shear panels with welded stiffeners", *Comput. Struct.*, **86**(6), 545-555.

Engelhardt, M.D. and Popov, E.P. (1992), "Experimental performance of long links in eccentrically braced frames", *J. Struct. Eng.*, **118**(11), 3067-3088.

Fehling, E., Pauli, W. and Bouwkamp, J.G. (1992), "Use of vertical shear Link in eccentrically braced frames", *Proceedings of the 10th World Conference on Earthquake Engineering*, Madrid, Spain, July.

Hossain, Md.R., Ashraf, M. and Albermani, F. (2009), "Numerical evaluation of yielding shear panel device: A sustainable technique to minimize structural damages due to earthquakes", *Universitas 21 International Graduate Research Conference*, Melbourne-Brisbane, Australia, November-December, pp. 65-68.

Hossain, Md.R., Ashraf, M. and Albermani, F. (2011), "Numerical modelling of yielding shear panel device for passive energy dissipation", *Thin-Wall. Struct.*, **49**(8), 1032-1044.

IBC (2012), International building code, International Code Council, Inc.; USA.

Miranda, E. (1993), "Site dependent strength reduction factor", *J. Struct. Eng., ASCE*, **119**(12), 3503-3519.

Özhendekci, D. and Özhendekci, N. (2008), "Effects of the frame geometry on the weight and inelastic behavior of eccentrically braced chevron steel frames", *J. Construct. Steel Res.*, **64**(3), 326-343.

Priestly, M.J.N., Seible, F. and Clavi, G.M. (1996), *Seismic Design and Retrofit of Bridges*, John Wiley and

Sons, New York, NY, USA.
Rai, D.C., Annam, P.K. and Pradhan, T. (2013), “Seismic testing of steel braced frames with aluminum shear yielding dampers”, *Eng. Struct.*, **46**, 737-747.
Saedi Daryan, A., Bahrampoor, H., Ziaei, M., Golafshar, A. and Assareh M.A. (2008), “Seismic behavior of vertical shear link made of easy-going steel”, *Am. J. Eng. Appl. Sci.*, **1**(4), 368-377.
Williams, M.S. and Albermani, F. (2003), “Monotonic and cyclic tests on shear diaphragm dissipators for steel frames”, *Civil Eng. Res. Bulletin*, No. 23, pp. 1-34.
Zahrai, S.M. and Bruneau, M. (1999), “Cyclic testing of ductile end diaphragm for slab-on-girder steel bridges”, *J. Struct. Eng., ASCE*, **125**(9), 987-996
Zahrai, S.M. and Moslehi Tabar, A. (2013), “Analytical study on cyclic behavior of chevron braced frames with shear panel system considering post-yield deformation”, *Can. J. Civil Eng.*, **40**(7), 633-643.

DL